Implementation of Single Fluid Volume Element Method in Predicting Flow Occurrence of One-Dimensional Geothermal Well

S. Viridi[1,*] and Y. Windra[2]

[1]Nuclear Physics and Biophysics, Faculty of Mathematics and Natural Science, Institut Teknologi Bandung, Jl. Ganesha 10. Bandung 40132, Indonesia

[2]Geothermal Engineering, Faculty of Mining and Petroleum Engineering, Institut Teknologi Bandung, Jl. Ganesha 10. Bandung 40132, Indonesia

[*]dudung@fi.itb.ac.id

Abstract

A finite difference based method known as single fluid volume element method (SFVE) is implemented into a simplified model of geothermal well. Two cases are discussed, where the former is when the well can not flow fluid and the later is when it can. In both cases the feed zone has the same 20 kg/s mass flow, but different shallow water temperature 40 & 70 °C, and pressure 1.0 & 5.4 MPa. There are two adjustable simulation parameters Δt and Δh which stand for time discretization and water volume element thickness, respectively. Influence of both parameters is discussed in the two cases for $\Delta t = 10^{-1}, 10^{-2}, .., 10^{-7}$ and $\Delta h = 1, 2, .., 64$. It is observed that each case has different numerical property to be aware of.

Keywords: finite difference, fluid flow, transient flow, geothermal well.

PACS: 47.27.nf, 47.60.-i, 91.40.Ge.

Introduction

A geothermal well can discharge by itself or it requires stimulation in several ways [1]. A one-dimensional model is constructed to simulate transient flow of a geothermal well, which is based on single fluid volume element method (SFVE) [2]. Proposed model reduces dimension in radial direction [3], but extends the profile in longitudinal direction of the flow. Several factors are not considered, such as fluid inclusion [4], evolution of natural reservoir [5], hydrothermal circulation [6], and two-phase flow [7], only for the sake of simplification.

Simulation

SFVE method is a finite difference based method, which is used to solve equation of motion of a single fluid volume element. This element represents transient motion of the fluid along its channel. Details of illustration and derivation of this method for vertical, horizontal, inclined, and semi-circular pipes can be found in [2], while only required equations presented in this work.

The element will have pressure force from fluid above and below it

$$F_p = \rho g\left[\left(z+\Delta h\right)-z\right]A\Delta h\,, \quad (1)$$

where A is well cross section, Δh thickness of the element, z position of the element, and ρ is fluid density, which is in general

$$\rho\left(T,p\right)=\frac{\rho_0}{\left[1+\beta\left(T-T_0\right)\right]\ \left[1-\left(p-p_0\right)/E\right]}, \quad (2)$$

with $\rho_0 = 1$ kg/m^3, $E = 2.15$ GPa, $p_0 = 1.023\times10^5$ Pa, $\beta = 2\times10^{-4}$ m^3/m$^3\cdot$°C, $T_0 = 0$ °C. Temperature and pressure are also function of depth z, which are provided by temperature- and pressure-depth profile.

There is also force due pressure drop related to position of the element relative to initial position of shallow water column z_0

$$F_d = \rho g\left(z-z_0\right). \quad (3)$$

Gravitation plays also a role to the element through

$$F_g = -\rho g A\Delta h\,. \quad (4)$$

The last considered force is viscous drag between the element and its channel

$$F_v = -8\pi\eta\Delta h v\,. \quad (5)$$

as in [8], which is modified from [9]. Fluid viscosity η is also function of temperature

$$\eta\left(T\right)=\eta_0\times10^{247.8/\left(T-140\right)}, \quad (6)$$

with $\eta_0 = 2414$ cP. Other forms [10] of Equation (6) can also be used.

Then using Newton second law of motion, acceleration of fluid element

$$a=\frac{1}{\rho A\Delta t}\left(F_p+F_d+F_g+F_v\right). \quad (7)$$

Integration of Equation (7) will produce velocity, and late integration will produce position. Numerical method used is simple Euler method

$$v(t+\Delta t) = v(t) + a(t)\Delta t \qquad (8)$$

and

$$z(t+\Delta t) = z(t) + v(t)\Delta t \; . \qquad (9)$$

Iteration though Equations (1) - (9) from initial time to final time will give transient dynamics of fluid element with thickness Δh.

Two termination conditions can be implemented, which $z > z_{\text{well head}}$ for dischargeable well and $v < \varepsilon$ for undischargeable well.

Well properties

Data from two different wells are used in this work for testing the simulation, where PAL-1RD represents successful well and PAL-9D represents failed well [11]. Figures 1 and 2 show profiles of temperature- and pressure-depth for both well. Details of data are also given in Appendix A.

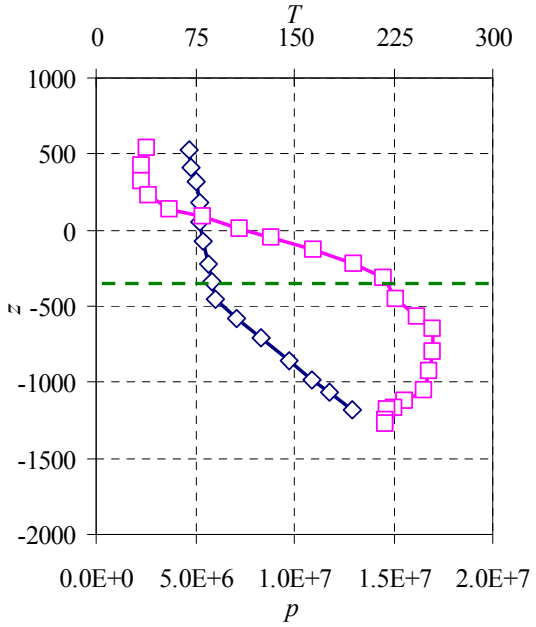

Figure 1. Profile of temperature(□)- and pressure(◊)-depth of PAL-1RD well, with position of shallow water column indicated by dashed line.

The PAL-1RD well has shallow water position at about -350 m, temperature about 40 °C, pressure of 1 MPa, and it fails to discharge, where PAL-9D well has shallow water position at about 200 m, temperature about 70 °C, pressure of 5.4 MPa, and it is successful to discharge.

Data obtained from Figures 1 and 2 will be used to develop interpolation functions for pressure and temperature as function of depth z, which are $p(z)$ and $T(z)$. Method used in the interpolation functions is simply linear interpolation.

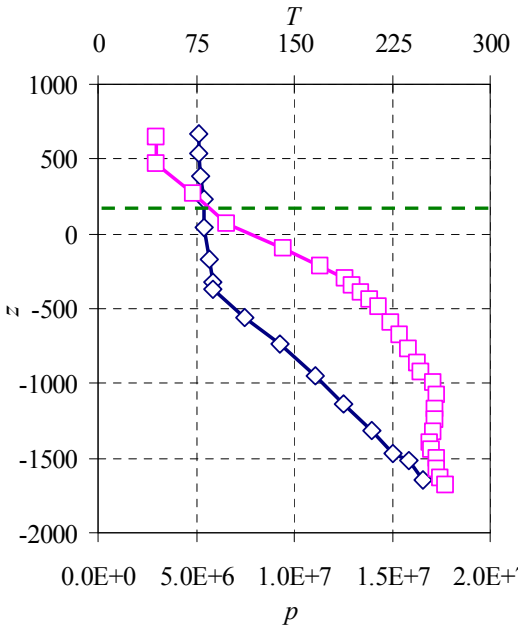

Figure 2. Profile of temperature(□)- and pressure(◊)-depth of PAL-9D well, with position of shallow water column indicated by dashed line.

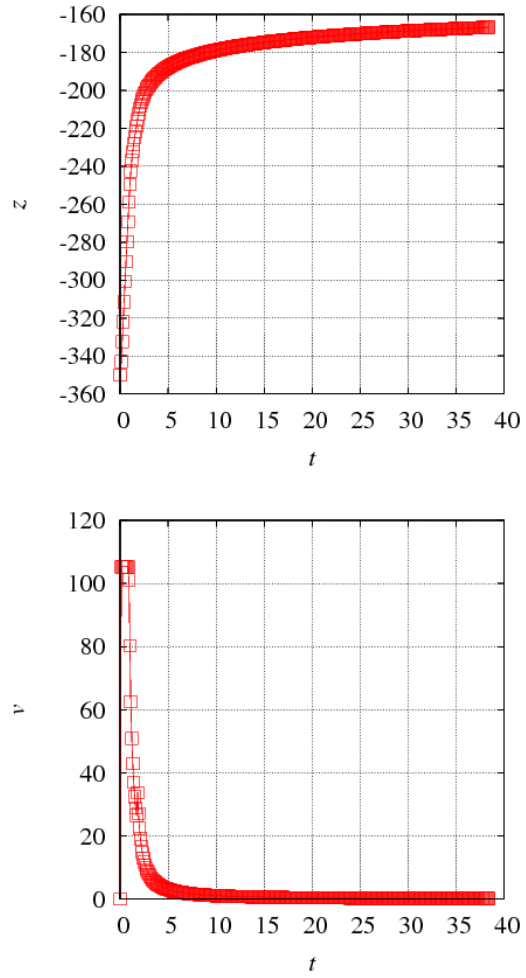

Figure 3. Fluid element position z (top) and velocity v (bottom) as function of time t for PAL-1RD well.

Results and discussion

A program named `gws1d` is built using previous mentioned equations. All simulation parameters are described in `PAL-1RD.txt` and `PAL-9D.txt` text files. How to run the program with both parameters file are given in Appendix B.

In general, parameters used are $\varepsilon = 10^{-8}$, $\Delta t = 10^{-4}$ s, $\Delta h = 1$ m, $T_{show} = 1$ s, $T_{end} = 200$ s, g = 9.81 m/s, $D_{well} = 0.5$ m, unless others are specified.

Case of unrechargeable well

Begin from depth of $z =$ 350 m, fluid element starts moving and reaches maximum height about -167 m, which is still less than well head position at 550 m. Simulation predicts that this well can not recharge as observed in the field [11].

Position and velocity of fluid element for PAL-1RD well in Figure 3 show consistency, where final position is reached as velocity goes to zero. Clearer picture of this can be seen in Figure 4.

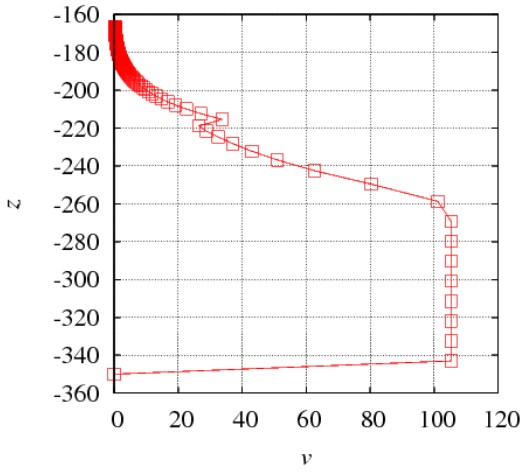

Figure 4. Fluid element position z againts velocity v or PAL-1RD well.

From z = -350 m fluid element starts moving and increases its speed, after some maximum speed, which is limited by mass flow of feed zone, it reduces it speed due to viscous drag and pressure drop. Then, its speed tends to decay as it approaches maximum position z_{max}, which is still much lower than well head position $z_{well\ head}$ = 550 m in this case.

A knick at about z = -215 m is still unexplained, but it could be discontinuity of $T(z)$ and $p(z)$ from interpolation functions.

Case of rechargeable well

In this case fluid element begins to flow from position z = 200 m. It accelerates and then seems to reach a terminal velocity about 106 m/s as it is shown in Figure 5. This behavior is rather different than in previous case.

How the relation between fluid element velocity and its position is given in Figure 6. Since well head position is about 682 m and fluid element can reach this position with non-zero velocity, then simulation predicts that PAL-9D can discharge, as it is observed in the field [11].

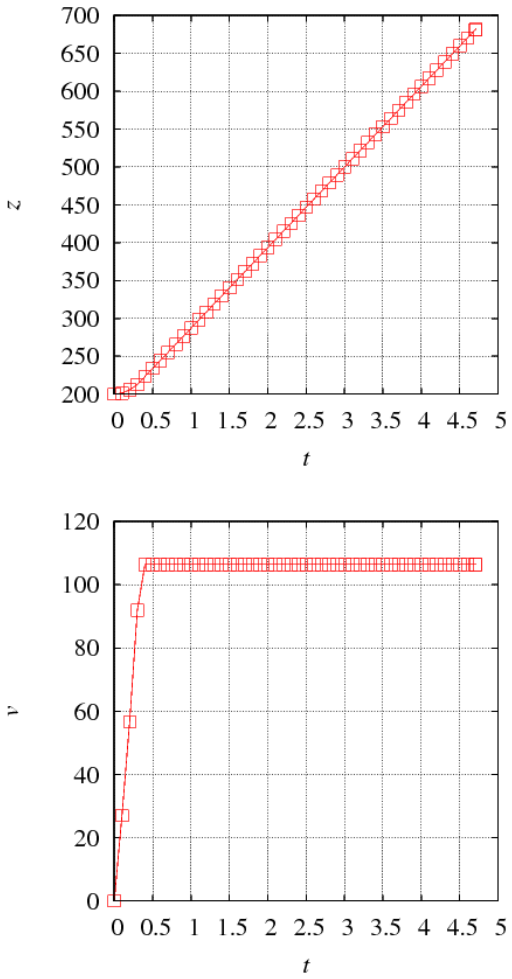

Figure 5. Fluid element position z (top) and velocity v (bottom) as function of time t for PAL-9D well.

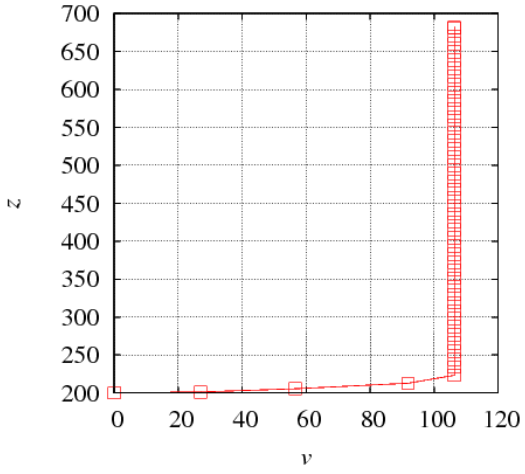

Figure 6. Fluid element position z againts velocity v or PAL-9D well.

It can be summarized until now that SFVE method is confirmed with observed data in predicting whether a well can discharge or not.

Influence of Δh and Δt

Different value of Δ*h* and Δ*t* are used to show their influence in producing the results.

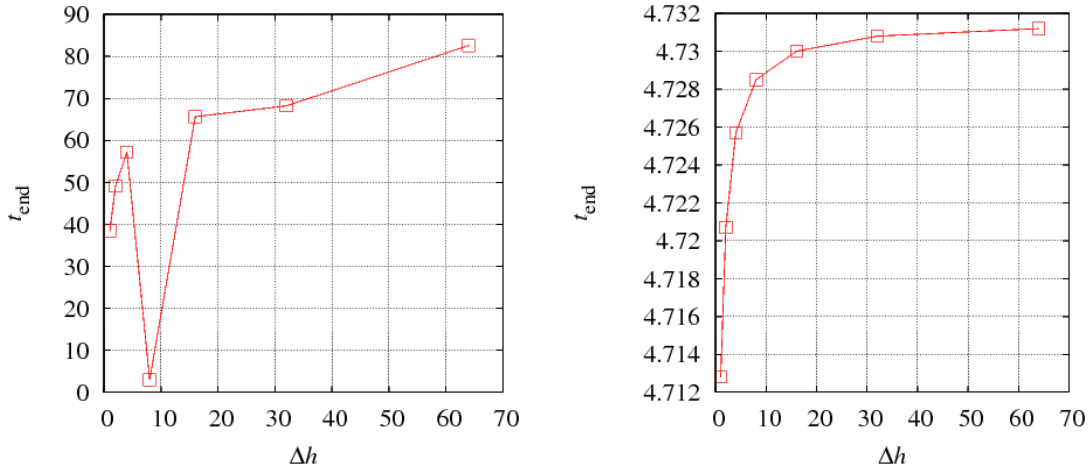

Figure 7. Influence of Δ*h* in determining value of t_{end} for the well of: PAL-1RD (left) and PAL-9D (right).

Figure 7 shows that for dischargeable well thicker Δ*h* gives more consistency results than for undischargeable well. Value of Δ*h* which is not so small is consistent as reported in [8], where are about 0.01 m for pipe with diameter about 0.6 mm and in this work Δ*h* > 60 m for diameter about 50 cm. Both results show that Δ*h* > *D*.

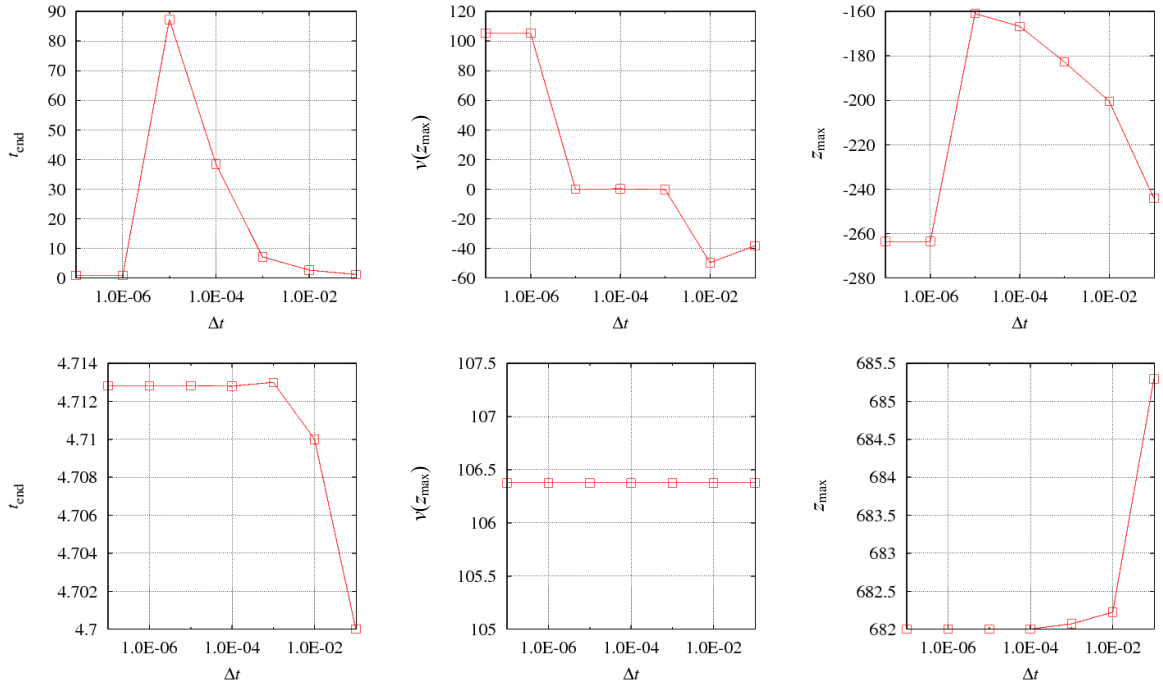

Figure 8. Influence of Δ*t* in determining value of t_{end}, $v(z_{max})$, and z_{max} (in left, center, and right column, respectively) for the well of: PAL-1RD (top row) and PAL-9D (bottom row).

Figure 8 shows that smaller Δ*t* gives better and consistency results for dischargeable well but not for undischargeable one. This means that further investigation in determining Δ*h* and Δ*t* is required especially for the case of undischargeable well. This problem could be addressed to the different nature of termination condition in ending the simulation for undischargeable and dischargeable well.

Further work must also be considering the way how confirming time stamp of the fluid element, since there is no information available regarding this feature of the simulation. If it can be performed, then

the time required to stimulate a well until it discharges can also be predicted.

Conclusion

SFVE method has been successfully implemented in testing prediction of two cases of geothermal well, failed and successful case. All cases are predicted accordingly. Time information is still doubtable since there is no available information for confirmation.

Acknowledgements

SV would like to thank RIK ITB in year 2015 for supporting this work.

References

[1] C. H. Siega, V. S. Saw, R. P. Andrino Jr., and G. F. Cañete, "Well-to-Well Two Phase Injection using A 10in Diameter Line to Initiate Well Discharge in Mahanagdong Geothermal Field, Leyte, Philippines", Proceedings of the 7th Asian Geothermal Symposium, July 25-26, 2006, pp. 23-38.

[2] S. Viridi, Novitrian, Nuhayati, W. Hidayat, F. D. E. Latief, and F. P. Zen, "Development of Single Fluid Volume Element Method for Simulation of Transient Fluid Flow in Self-Siphons", AIP Conference Proceedings 1615, 199-207 (2014).

[3] Z. Deng, S. J. Rees, and J. D. Spitler, "A Model for Annual Simulation of Standing Column Well Ground Heat Exchangers", International Journal of Heating, Ventilating, Air-Conditioning, and Refrigerating Research 11, 637-655 (2005).

[4] M. Sasada, E. Roedder, and H. E. Belkin, "Fluid Inclusions from Drill Hole DW-5, Hohi, Geothermal Area, Japan: Evidence of Boiling and Procedure for Estimating CO_2 Content", Journal of Volcanology and Geothermal Research 30, 231-251 (1986).

[5] G. Melosh, J. Moore, and R. Stacey, "Natural Reservoir Evolution in the TolhuacaGeothermal Field, Southern Chile", Proceedings of Thirty-Sixth Workshop on Geothermal Reservoir Engineering Stanford University, Stanford, California, January 30 - February 1, 2012, pp. SGP-TR-194 (7 pages).

[6] Y. Suzuki, S. Ioka, and H. Muraoka, "Determining the Maximum Depth of Hydrothermal Circulation using Geothermal Mapping and Seismicity to Delineate the Depth to Brittle-Plastic Transition in Northern Honshu, Japan", Energies 7, 3503-3511 (2014).

[7] H. Hossein-Pourazad, "High-Temperature Geothermal Well Design", Geothermal Training Programme, Reports 2005, Number 5, pp. 111-123.

[8] S. Viridi, Suprijadi, S. N. Khotimah, Novitrian, and F. Masterika, "Self-Siphon Simulation using Molecular Dynamics Method", Recent Development in Computational Science 2, 9-16 (2011).

[9] T. E. Faber, Fluid Dynamics for Physicist, Cambridge: University Press, 1995, pp. 227-232.

[10] C. J. Seeton, "Viscosity–Temperature Correlation for Liquids", Tribology Letters 22, 67-84 (2006).

[11] F. X. M. Sta. Ana, "A Study on Simulation by Air Compression on Some of the Philippine Geothermal Wells", Geothermal Institute, University of Auckland, Australia, October 1985.

Appendix A: Wells data

```
# Simulation parameters
DT      1E-4
TSHOW   0.1
TEND    200
DH      1
EPS     1E-8
VERBOSE 0

# Physical properties
GRAVITY 9.81
VISCOSITY       1E-2

# Well information
W_NAME  PAL-1RD
W_DATE  1984-01-00
W_STATUS        Failed
W_DIAMETER      0.5
W_HEAD  550.0

# Shallow water column
SWC_POSITION    -350.0
SWC_TEMPERATURE         40.0
SWC_PRESSURE    1.0E6

# Feed zone
FZ_POSITION     -1450.0
FZ_THICKNESS    50.0
FZ_MASS_FLOW    20.0
FZ_TEMPERATURE 197.0
FZ_PRESSURE     11.4E6

# Air compress target
ACT_POSITION    -1100
ACT_TEMPERATURE         247
ACT_PRESSURE    1.18E7

# Interpolation data
```

```
DEPTH_PRESSURE_DATA    15
523.0   4.7E6
413.5   4.8E6
320.2   5.0E6
186.4   5.2E6
48.5    5.2E6
-77.2   5.4E6
-219.1  5.7E6
-332.7  5.8E6
-454.3  6.0E6
-576.0  7.1E6
-705.8  8.3E6
-859.9  9.7E6
-985.6  10.9E6
-1066.7 11.8E6
-1176.2 12.9E6

# Interpolation data
DEPTH_TEMPERATURE_DATA 22
541.0   38.2
425.5   34.8
315.6   34.8
227.6   39.9
139.6   55.5
84.6    80.6
7.7     109.2
-52.8   133.4
-135.3  164.6
-217.8  195.7
-311.3  218.2
-454.2  226.9
-569.7  243.3
-652.1  254.6
-795.1  254.6
-921.6  252.0
-1053.5 247.6
-1125.0 233.8
-1169.0 226.0
-1180.0 219.9
-1246.0 219.1
-1273.5 219.1


# Simulation parameters
DT      1E-4
TSHOW   0.1
TEND    200
DH      1
EPS     1E-8
VERBOSE 0

# Physical properties
GRAVITY 9.81
VISCOSITY      1E-2

# Well information
W_NAME  PAL-9D
W_DATE  1984-10-00
W_STATUS       Success
W_DIAMETER     0.5
W_HEAD  682.0

# Shallow water column
SWC_POSITION   200.0
SWC_TEMPERATURE        70.0
SWC_PRESSURE   5.4E6

# Feed zone
FZ_POSITION    -1350.0
FZ_THICKNESS   100.0
FZ_MASS_FLOW   20.0
FZ_TEMPERATURE 254.0
FZ_PRESSURE    13.3E6

# Air compress target
ACT_POSITION   -400
ACT_TEMPERATURE        200
ACT_PRESSURE   6.0E6

# Interpolation data
DEPTH_PRESSURE_DATA    16
671.2   5.1E6
544.5   5.1E6
389.0   5.2E6
233.4   5.4E6
49.1    5.45E6
-169.8  5.7E6
-319.5  5.9E6
-365.6  5.9E6
-555.7  7.5E6
-740.0  9.3E6
-953.1  11.1E6
-1143.2 12.5E6
-1316.0 14.0E6
-1465.8 15.0E6
-1517.6 15.9E6
-1644.3 16.6E6

# Interpolation data
DEPTH_TEMPERATURE_DATA 27
646.4   44.1
464.4   44.8
268.0   73.5
71.6    99.2
-100.8  141.5
-210.9  170.1
-301.9  189.0
-345.0  194.3
-397.7  201.1
-440.8  207.9
-483.9  214.7
-598.9  224.5
-675.5  231.3
-766.5  237.3
-871.8  244.9
-929.3  247.9
```

```
-991.6  256.2
-1082.6 259.2
-1173.6 257.7
-1240.6 257.7
-1322.0 256.9
-1393.9 254.7
-1446.6 255.4
-1504.0 259.2
-1580.7 260.0
-1628.5 262.2
-1676.4 266.8
```

Appendix B: How to execute `gws1d` code

```
./gws1d PAL-1RD.txt
./gws1d PAL-9D.txt
```